Variation of Helical Pitches Driven by the Composition of *N*-Propargylamide Copolymers

Jianping Deng, Junichi Tabei, Masashi Shiotsuki, Fumio Sanda,* and Toshio Masuda*

Department of Polymer Chemistry, Graduate School of Engineering, Kyoto University, Katsura Campus, Kyoto 615-8510, Japan

Received September 7, 2004; Revised Manuscript Received October 4, 2004

ABSTRACT: Five novel *N*-propargylacetamide and -propaneamide monomers [HC≡CCH_2NHCOR; **4**: R = $CH_2C_6H_5$, **5**: R = $CH(C_6H_5)_2$, **6**: R = $CH_2CH_2C_6H_5$, **7**: R = $CH_2CH(C_6H_5)_2$, **8**: R = $CH_2C(C_6H_5)_3$] were polymerized with a rhodium catalyst, $(nbd)R^+B^-(C_6H_5)_4$ (nbd = 2,5-norbornadiene), to provide polymers in 81−99% yields. Poly(**4**), poly(**5**), and poly(**8**) possessed low molecular weights (M_n = 3100−6100), presumably due to their low solubility in solvents, while poly(**6**) and poly(**7**) had moderate M_n's (15 000 and 16 700) and good solubility in several solvents including chloroform. The secondary structures of the five polymers in chloroform were investigated by UV−vis spectroscopy. Poly(**4**) adopted a helical structure to a certain extent, while poly(**5**)−poly(**7**) hardly did not. In contrast, poly(**8**) exhibited a UV−vis absorption peak around 365 nm, demonstrating that it invariably formed helices under the given conditions. Copolymers of monomer **8** with either chiral monomer **10** [HC≡$CCH_2NHCOCH(CH_3)CH_2CH_3$] or achiral monomers **1** [HC≡$CCH_2NHCOC(CH_3)_2C_6H_5$] and **9** [HC≡$CCH_2NHCO(CH_2)_5CH_3$], i.e., poly(**8**-*co*-**10**)s, poly(**8**-*co*-**1**)s, and poly(**8**-*co*-**9**)s, showed good solubility and possessed higher M_n's than that of poly(**8**). Furthermore, with the increase of unit **8** in poly(**8**-*co*-**10**)s, poly(**8**-*co*-**1**)s, and poly(**8**-*co*-**9**)s, initial blue and then red shifts were observed in the λ_{max} of their UV−vis spectra and further in the CD signal of poly(**8**-*co*-**10**)s, demonstrating that all of these copolymers formed helices with different pitches, which depended on the compositions of the copolymers. Additionally, the sergeants and soldiers rule was observed in achiral/chiral poly(**8**-*co*-**10**)s.

Introduction

In recent years, conjugated polymers are intensively studied mainly because of their interesting electrical and optical properties and, more importantly, their potential utility in electronic and photonic applications.[1] Among these polymers, those with the ability to adopt helical structures are especially of great importance since they might perform circularly polarized electroluminescence behavior under suitable conditions and can be developed as data storage and display materials and thus are more attractive.[2] In addition, in macro- and supramolecular chemistry, control of helicity draws much attention since polymers with controllable higher order structures are applicable to stimuli-responsive materials[3] and enantioselective catalysts[4] as well. It has been known that biomacromolecules, such as proteins and DNA, can adopt helical structures which are stabilized by intramolecular hydrogen bonds.[5] Inspired by this elegant feature of nature, a great number of studies have been devoted so far to the development of synthetic polymers that can adopt helical structure.[6]

A large body of our earlier work has revealed that both intramolecular hydrogen bonding and steric repulsion between the pendent groups are the factors for poly(*N*-propargylamides) to form stable helices.[7] Poly(*N*-propargylamides) having pendent groups with moderate lengths can adopt helical structure at room temperature, while poly(*N*-propargylamides) with too short or too long pendent groups take helical form only at low temperature or hardly form helices under the same experimental conditions.[7a,b] Poly(*N*-propargylamides) with bulky pendent groups can take dynamically stable helices.[7c] However, too bulky pendent groups exert adverse effects on the stability of the resulting helices, which is evidently exemplified by poly(**1**)−poly(**3**) in Scheme 1.[7j] Poly(**1**) takes stable helices even at 60 °C due to the appropriate steric repulsion between the pendent groups, while either poly(**2**) or poly(**3**) cannot under the similar conditions. Poly(**2**-*co*-**9**)s with unit **9** higher than 25% can adopt helical structure, presumably because the steric repulsion between the pendent

Scheme 1

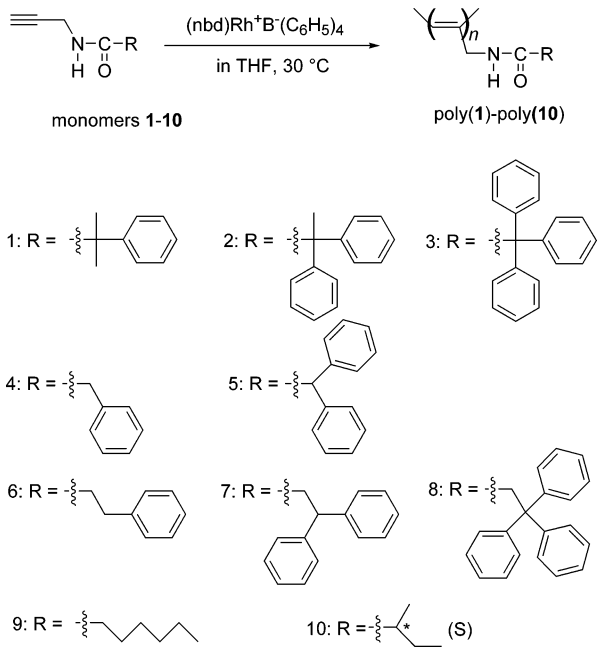

* Corresponding authors: Tel +81-75-383-2589; Fax +81-75-383-2590; e-mail sanda@adv.polym.kyoto-u.ac.jp, masuda@adv.polym.kyoto-u.ac.jp.

10.1021/ma048177r CCC: $27.50
Published on Web 11/24/2004

groups is operatively reduced by copolymerization. In contrast, only poly(**3**-*co*-**9**)s having unit **9** more than 90% can take helical structure, indicating that the bulkiness of unit **3** cannot be effectively reduced even by copolymerization.[7j]

The present article deals with the polymerization of a series of five novel phenyl-substituted *N*-propargylacetamides and -propaneamides **4**−**8** in Scheme 1 to obtain further insight into the effects of steric repulsion on the stability of the formed helices. We further examined the copolymerization of monomer **8** with monomers **10**, **1**, and **9** to improve the solubility, increase the molecular weight of poly(**8**), and elucidate the effects of compositions on the contents and pitches of the helices in the copolymers. It was found that all the copolymers, poly(**8**-*co*-**10**)s, poly(**8**-*co*-**1**))s, and poly(**8**-*co*-**9**)s, can adopt helices with different pitches depending on the compositions of the copolymers.

Experimental Section

Measurements. Melting points (mp) were measured by a Yanaco micro melting point apparatus. Elemental analysis was carried out at the Kyoto University Elemental Analysis Center. The number- and weight-average molecular weights (M_n and M_w) and molecular weight distributions (M_w/M_n) of (co)polymers were determined by GPC (Shodex KF-850 column) calibrated with polystyrenes as standards and THF or chloroform as an eluent. UV−vis spectra were recorded on a JASCO J-820 spectropolarimeter. ^{1}H and ^{13}C NMR spectra were recorded on a JEOL EX-400 spectrometer. IR spectra were recorded with a Shimadzu FTIR-8100 spectrophotometer.

Materials. THF as a polymerization solvent was distilled by the standard method. Propargylamine (TCI), phenylacetyl chloride (TCI), diphenylacetic acid (Aldrich), 3-phenylpropionic acid (TCI), 3,3-diphenylpropionic acid (TCI), 3,3,3-triphenylpropionic acid (TCI), thionyl chloride (Wako), pyridine (Wako), isobutyl chloroformate (Wako), and 4-methylmorpholine (Wako) were used as received. (nbd)Rh$^+$B$^-$(C_6H_5)$_4$ catalyst was prepared as reported.[8]

Monomer Synthesis. Syntheses of monomers **1**−**3**,[7j] **9**,[7a] and **10**[7g] were reported in the preceding papers. Monomer **4** was synthesized according to the method reported earlier.[7h] Monomers **5**, **7**, and **8** were synthesized with the method reported in the preceding article.[7j] Monomer **6** was synthesized according to the method introduced previously.[7a] Monomers **4**−**8** are new compounds. Now, taking the syntheses of monomers **4**, **6**, and **8** as examples, the main synthetic procedures of the three different methods are described. Monomer **4**: phenylacetyl chloride (5.0 mL, 38.0 mmol), pyridine (6.1 mL, 76.0 mmol), and propargylamine (5.2 mL, 76 mmol) were added to ether (200 mL) sequentially. The solution was stirred first at 0 °C and then at room temperature (rt) for 24 h. Afterward, the precipitate formed was filtered off, and the filtrate was collected, which was washed with 2 M HCl three times and then with saturated aqueous $NaHCO_3$ to neutralize the solution. Then, the solution was dried over anhydrous $MgSO_4$, filtered, and concentrated by removing the solvents with rotary evaporation to give the target monomer. The crude monomer was purified by flash column chromatography on silica gel (hexane/ethyl acetate = 1/1, v/v). Monomer **6**: 3-phenylpropionic acid (5.0 g, 33.0 mmol), isobutyl chloroformate (4.3 mL, 33.0 mmol), and 4-methylmorpholine (3.6 mL, 33.0 mmol) were added to THF (200 mL) sequentially. The solution was stirred at rt for 10 min, and then propargylamine (2.3 mL, 33.0 mmol) was added to the solution. After 1 h, white precipitate formed was filtered off, and the filtrate was collected, to which ethyl acetate (ca. 50 mL) was added to extract the desired product. The combined solution was washed with 2 M HCl three times and then washed with saturated aqueous $NaHCO_3$ to neutralize the solution. Then, the solution was dried over anhydrous $MgSO_4$, filtered, and concentrated to give the target monomer. The crude monomer was purified by flash column chromatography on silica gel (hexane/ethyl acetate = 1.5/1, v/v). Monomer **8**: 3,3,3-triphenylpropionic acid (5.0 g, 16.6 mmol) was added to thionyl chloride (11.9 mL, 166.0 mmol), and the solution was refluxed for 3 h. The residual thionyl chloride was removed by rotatory evaporation, and the product was added to ethyl ether (200 mL). After the product completely dissolved, pyridine (2.7 mL, 33.1 mmol) and propargylamine (2.3 mL, 33.1 mmol) were sequentially added to the solution. The solution was stirred at 0 °C for 2 h, and then the white precipitate formed was filtered off. The filtrate was washed with 2 M HCl three times and then with saturated aqueous $NaHCO_3$ to neutralize the solution. Afterward, the solution was dried over anhydrous $MgSO_4$, filtered, and concentrated to give the target monomer. The crude monomer was purified twice by flash column chromatography on silica gel (hexane/ethyl acetate = 3/1, v/v). Monomers **5** and **7** were prepared by a similar method for monomer **8** from the corresponding carboxylic acids. The data of monomers **4**−**8** are as follows:

Monomer **4**: yield 53%, pale yellow crystal, mp 77−78 °C. IR (KBr): 3294 (H−N), 2360 (H−C≡), 1649 (C═O), 1507, 694 (phenyl), 1555, 1227, 669, 684 cm^{-1}. ^{1}H NMR ($CDCl_3$, 400 MHz, 22 °C): δ 2.18 (s, 1H, *CH*≡C), 3.59 (s, 2H, *CH*$_2$Ph), 4.01 (s, 2H, CH≡C*CH*$_2$), 5.97 (broad s, 1H, N*H*), 7.19−7.25 (m, 5H, Ph−*H*).^{13}C NMR ($CDCl_3$, 400 MHz, 22 °C): δ 29.24, 43.00, 71.43, 79.35, 127.31, 128.90 (×2), 129.32 (×2), 134.33, 170.62. Anal. Calcd for $C_{11}H_{11}NO$: C, 76.28; H, 6.40; N, 8.09. Found: C, 76.10; H, 6.50; N, 8.06. Monomer **5**: yield 49%, white solid, mp 131−132 °C. IR (KBr): 3292 (H−N), 2370 (H−C≡), 1648 (C═O), 1507, 694 (phenyl), 1556, 1449, 1270, 609, 550 cm^{-1}. ^{1}H NMR ($CDCl_3$, 400 MHz, 22 °C): δ 2.19 (s, 1H, *CH*≡C), 4.08 (s, 2H, CH≡C*CH*$_2$), 4.93 (s, 1H, *CHPh*$_2$), 5.81 (broad s, 1H, N*H*), 7.14−7.25 (m, 10H, Ph−*H*).^{13}C NMR ($CDCl_3$, 400 MHz, 22 °C): δ 29.54, 58.83, 71.71, 79.25, 127.34 (×2), 128.78 (×4), 128.82 (×4), 138.97 (×2), 171.48. Anal. Calcd for $C_{17}H_{15}NO$: C, 81.90; H, 6.06; N, 5.62. Found: C, 81.77; H, 6.09; N, 5.63. Monomer **6**: yield 60%, colorless crystal, mp 61−63 °C. IR (KBr): 3278 (H−N), 2382 (H−C≡), 1636 (C═O), 1508, 702 (phenyl), 1540, 1236, 1020, 679, 650 cm^{-1}. ^{1}H NMR ($CDCl_3$, 400 MHz, 22 °C): δ 2.19 (s, 1H, *CH*≡C), 2.47 (s, 2H, *CH*$_2$CH$_2$-Ph), 2.95 (s, 2H, CH$_2$*CH*$_2$Ph), 3.96 (s, 2H, CH≡C*CH*$_2$), 5.97 (broad s, 1H, N*H*), 7.14−7.20 (m, 5H, Ph−*H*).^{13}C NMR ($CDCl_3$, 400 MHz, 22 °C): δ 29.08, 31.46, 38.01, 71.42, 79.46, 126.18, 128.21 (×2), 128.44 (×2), 140.55, 171.80. Anal. Calcd for $C_{12}H_{13}NO$: C, 76.98; H, 7.00; N, 7.48. Found: C, 77.13; H, 7.05; N, 7.47. Monomer **7**: yield 55%, pale yellow crystal, mp 110−111 °C. IR (KBr): 3297 (H−N), 2395 (H−C≡), 1636 (C═O), 1508, 706 (phenyl), 1540, 1238, 1040, 745, 611, 566 cm^{-1}. ^{1}H NMR ($CDCl_3$, 400 MHz, 22 °C): δ 2.17 (s, 1H, *CH*≡C), 2.92 (s, 2H, *CH*$_2$CHPh$_2$), 3.92 (s, 2H, CH≡C*CH*$_2$), 4.60 (s, 1H, CH$_2$*CHPh*$_2$), 5.74 (broad s, 1H, N*H*), 7.15−7.24 (m, 10H, Ph−*H*).^{13}C NMR ($CDCl_3$, 400 MHz, 22 °C): δ 29.08, 42.89, 47.16, 71.40, 79.27, 126.49 (×2), 127.62 (×4), 128.52 (×4), 143.43 (×2), 170.73. Anal. Calcd for $C_{18}H_{17}NO$: C, 82.10; H, 6.51; N, 5.32. Found: C, 82.05; H, 6.54; N, 5.29. Monomer **8**: yield 50%, white crystal, mp 145−146 °C. IR (KBr): 3312 (H−N), 2395 (H−C≡), 1637 (C═O), 1508, 704 (phenyl), 1492, 1238, 1156, 1036, 745, 612, 566 cm^{-1}. ^{1}H NMR ($CDCl_3$, 400 MHz, 22 °C): δ 2.03 (s, 1H, *CH*≡C), 3.53 (s, 2H, *CH*$_2$CPh$_3$), 3.66 (s, 2H, CH≡C*CH*$_2$), 4.38 (broad s, 1H, N*H*), 7.15−7.24 (m, 15H, Ph−*H*).^{13}C NMR ($CDCl_3$, 400 MHz, 22 °C): δ 29.18, 48.52, 56.22, 71.25, 78.99, 126.51 (×3), 128.11 (×6), 129.07 (×6), 146.00 (×3), 170.15. Anal. Calcd for $C_{24}H_{21}NO$: C, 84.92; H, 6.24; N, 4.13. Found: C, 84.62; H, 6.15; N, 3.97.

Polymerization and Copolymerization. All (co)polymerizations were carried out with (nbd)Rh$^+$B$^-$(C_6H_5)$_4$ as a catalyst in dry THF at 30 °C for 1 h under the following conditions unless otherwise stated: [monomer]$_0$ = 0.60 M, [catalyst] = 6 mM. After polymerization, the reaction mixture was poured into a large amount of hexane to precipitate the formed (co)polymer. Then, the (co)polymer was filtered off, washed with hexane, and dried under reduced pressure. In the case of copolymerization, the total monomer concentration was kept 0.6 M, while other conditions were the same as for homopolymerization. We assumed that the compositions of the

Table 1. Polymerization of Monomers 4−8[a]

monomer	yield[b] (%)	M_n[c]	M_w/M_n[c]	cis content[d] (%)
4	83[e]	6100	2.13	n.d.[f]
5	81[e]	5500	2.37	n.d.[f]
6	99	16700	1.96	100
7	96	15000	2.01	100
8	97[e]	3100	1.29	n.d.[f]

[a] With (nbd)$Rh^+B^-(C_6H_5)_4$ catalyst in THF at 30 °C for 1 h; [M] = 0.60 M; $[M]_0/[Rh] = 100$. [b] Precipitated in hexane. [c] Measured by GPC (polystyrenes as the standards; $CHCl_3$ as an eluent). [d] Determined by ^1H NMR in $CDCl_3$ at 50 °C. [e] Partly soluble (more than 85%) in chloroform. [f] Could not be determined because of broad signals.

Table 2. Solubility of Poly(4)−Poly(8)[a]

solvent	poly(**4**)	poly(**5**)	poly(**6**)	poly(**7**)	poly(**8**)
toluene	×	×	□	○	×
THF	□	□	○	○	□
$CHCl_3$	□	□	○	○	□
DMF	×	×	○	○	×
DMSO	×	×	○	○	×
MeOH	×	×	□	×	×

[a] ×, insoluble; □, partly soluble; ○ soluble; polymer sample 2 mg/solvent 1 mL; determined at rt.

copolymers were identical to the corresponding monomer feeds because the copolymer yields were practically quantitative in all cases. Spectroscopic data of poly(**4**)−poly(**8**) are as follows: Poly(**4**): IR (KBr): 3290 (H−N), 2350 (H−C═), 1654 (C═O), 1507, 695 (phenyl), 1560, 1230, 745 cm^{-1}. ^1H NMR ($CDCl_3$, 400 MHz, 50 °C): δ 1.49 (s, 2H, CH_2Ph), 4.04 (s, 2H, C═CCH_2), 5.67 (broad s, 1H, *CH*═C), 7.30−7.60 (m, 5H, Ph−*H*), 7.76 (broad s, 1H, N*H*). Poly(**5**): IR (KBr): 3290 (H−N), 2372 (H−C═), 1654 (C═O), 1508, 697 (phenyl), 1560, 1473, 1229, 1032, 744, 643, 537 cm^{-1}. ^1H NMR ($CDCl_3$, 400 MHz, 50 °C): δ 1.50 (s, 1H, *CH*Ph_2), 4.07 (s, 2H, CH═CCH_2), 5.66 (broad s, 1H, *CH*═C), 7.25−7.65 (m, 10H, Ph−*H*), 7.80 (broad s, 1H, N*H*). Poly(**6**): IR (KBr): 3275 (H−N), 2380 (H−C═), 1637 (C═O), 1508, 698 (phenyl), 1540, 1256, 1029, 698 cm^{-1}. ^1H NMR ($CDCl_3$, 400 MHz, 50 °C): δ 2.10−2.30 (m, 4H, CH_2CH_2Ph), 3.97 (s, 2H, CH═CCH_2), 5.62 (s, 1H, *CH*═C), 7.10−7.50 (m, 6H, N*H*, Ph−*H*). Poly(**7**): IR (KBr): 3295 (H−N), 2392 (H−C═), 1648 (C═O), 1508, 698 (phenyl), 1540, 1240, 1031, 745, 611 cm^{-1}. ^1H NMR ($CDCl_3$, 400 MHz, 50 °C): δ 1.64 (m, 2H, CH_2CHPh_2), 3.08 (broad s, 2H, CH═CCH_2), 4.61 (s, 1H, CH_2*CH*Ph_2), 5.02 (broad s, 1H *CH*═C), 7.13−7.40 (m, 10H, Ph−*H*), 8.27 (broad s, 1H, N*H*). Poly(**8**): IR (KBr): 3298 (H−N), 2392 (H−C═), 1637 (C═O), 1508, 698 (phenyl), 1491, 1250, 1032, 668 cm^{-1}. ^1H NMR ($CDCl_3$, 400 MHz, 50 °C): δ 1.44 (s, 1H, CH_2CPh_3), 4.00 (s, 2H, CH═CCH_2), 5.64 (broad s, 1H, *CH*═C), 7.00−7.50 (m, 15H, Ph−*H*), 7.76 (broad s, 1H, N*H*).

Results and Discussion

Synthesis of Poly(4)−Poly(8). Table 1 shows that monomers **4**, **5**, and **8** provided polymers with low molecular weights (M_n = 3100−6100) in high yields (≥81%), while monomers **6** and **7** polymerized smoothly to give polymers with moderate M_n's (16 700 and 15 000, respectively) virtually quantitatively. Poly(**6**) and poly(**7**) were easily soluble in THF, chloroform, DMF, and DMSO, while poly(**4**), poly(**5**), and poly(**8**) were partly soluble in THF and chloroform as summarized in Table 2. This finding of solubility can be accounted for by considering that poly(**6**) and poly(**7**) have more flexible side groups than those of poly(**4**) and poly(**5**) and less bulky groups than that of poly(**8**). During the polymerization, the reaction mixtures of monomers **4**, **5**, and **8** became somewhat heterogeneous at different stages due to the poor solubility of the formed polymers. Rh catalysts predominantly afford polyacetylenes with cis structure.[9] The cis contents of the five polymers were

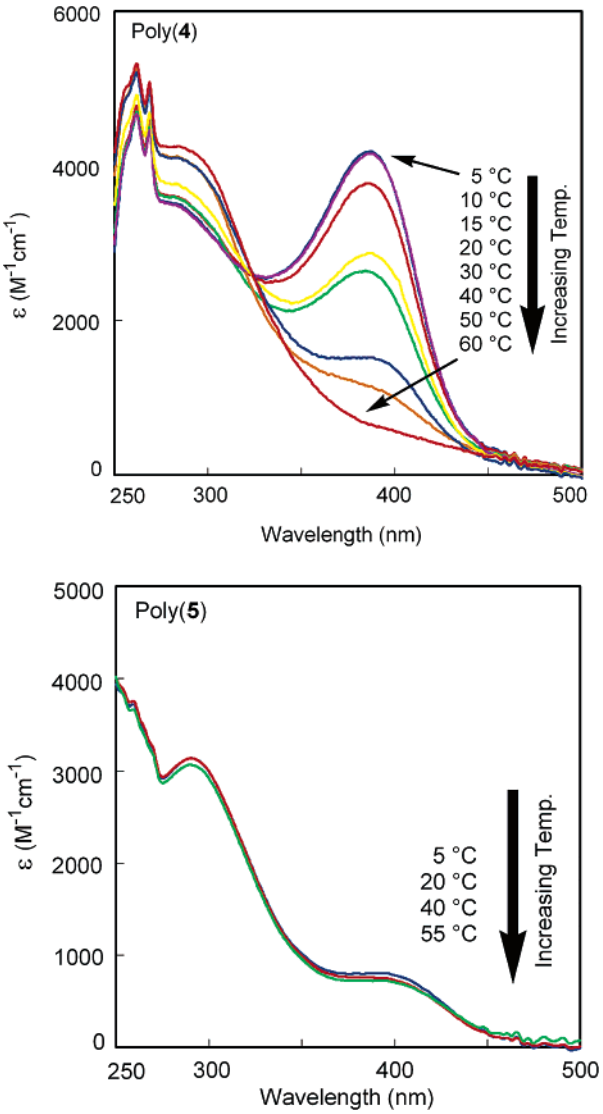

Figure 1. UV−vis spectra of poly(**4**) and poly(**5**) measured in $CHCl_3$ at 5−55 °C (c = 0.08−0.10 mM; $CHCl_3$-soluble part was used).

determined by ^1H NMR spectroscopy measured in chloroform-*d* at 50 °C.[7a] Both poly(**6**) and poly(**7**) had quantitative cis contents, while the cis contents of poly(**4**), poly(**5**), and poly(**8**) could not be determined because the signals of the olefinic protons appeared broadly. This should be because the crowded pendent groups of these polymers suppressed the mobility of the polymer main chains.

Secondary Structures of Poly(4)−Poly(8). The secondary structures of the five polymers were examined by UV−vis spectroscopy measured in chloroform, and the UV−vis spectra are illustrated in Figures 1 and 2. In the UV−vis spectra of poly(**4**) (Figure 1), there were two UV−vis absorption peaks around 300 and 400 nm. The intensity of the absorption peak around 400 nm gradually reduced as the temperature was raised from 5 to 60 °C, while the intensity of the absorption peak around 300 nm increased simultaneously. According to our earlier studies,[7] the absorption peaks around 300 and 400 nm originate from the random coil and helical structures, respectively, of poly(*N*-propargylamides). Therefore, it can be said that poly(**4**) can form helices in chloroform under appropriate conditions. However, even at 5 °C, the absorption peak at 300 nm

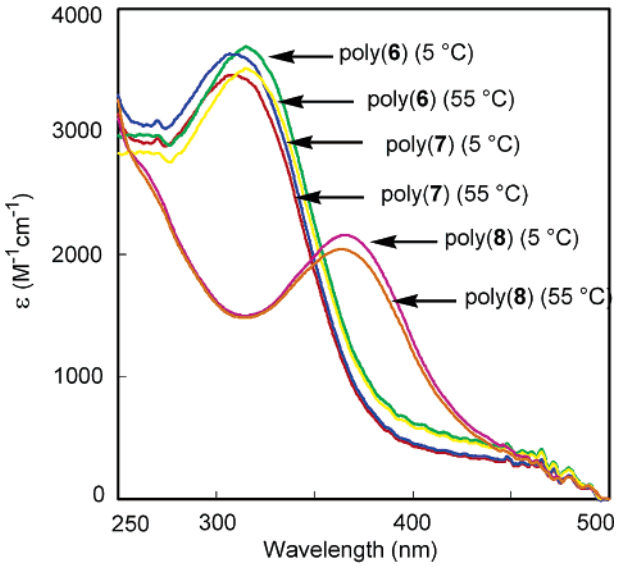

Figure 2. UV−vis spectra of poly(**6**)−poly(**8**) measured in $CHCl_3$ at 5 and 55 °C (c = 0.08−0.10 mM; $CHCl_3$-soluble part was used).

was still clearly observed, which means that only part of the polymer chains took helical structure. Moreover, when the temperature was lowered further, the absorption peaks at 300 and 400 nm hardly changed in magnitude, suggesting that the helical content became saturated at 5 °C. This phenomenon is different from those of previously examined poly(*N*-propargylamides),[7] in which the absorption peak around 300 nm totally disappears when the absorption peak around 400 nm becomes saturated. In poly(**5**), as depicted in Figure 1, the absorption peaks around 400 nm could be observed, but their intensities were quite low. Since we have already reported that no helix is found in poly(**3**),[7j] it can be concluded that the ability to form helices decreases in the sequence of poly(**4**) > poly(**5**) > poly(**3**). It is apparent that the pendent groups become bulky in the same sequence. These results mean that the steric repulsion between the pendent groups in poly(**5**) and poly(**3**) is too large, which prevents the polymers from adopting helical structure, while poly(**4**) carries less hindered pendent groups and can form helix at a high degree.

Figure 2 depicts the UV−vis spectra of poly(**6**)−poly(**8**). Poly(**6**) and poly(**7**) showed no UV−vis absorption peak around 400 nm but a large peak around 320 nm at 5−55 °C, indicating that they hardly adopt helix under the experimental conditions. Meanwhile, poly(**8**) exhibited an absorption peak around 365 nm, unlike the other poly(*N*-propargylamides) mentioned above. This peak slightly weakened as the temperature was raised from 5 to 55 °C. Since the sample solution was filtered twice with a filter (pore size 0.45 μm) before measurement, the UV−vis absorption peak around 365 nm should not be attributed to aggregates. Here, a hypothesis can be made that this peak stems from a helical structure formed in poly(**8**), which is verified in the following sections. In addition, we can assume that the helix of poly(**8**) is generated by not only the intramolecular hydrogen bonds and steric repulsion between the pendent groups but also hydrophobic interactions[10] between the neighboring phenyl groups in side chains.

Achiral/Chiral Copolymers, Poly(8-*co*-10)s. In the above section, it was assumed that the UV−vis absorption peaks of poly(**8**) in Figure 2 were attributable to the formation of helices. However, CD spectroscopic study is necessary to gain more information about the helical structure. Therefore, copolymerizations of achiral monomer **8** with chiral monomer **10** were performed, whose results are compiled in Table 3. The copolymerizations of monomers **8** and **10** proceeded smoothly to give the copolymers in high yields (96% and above). All the copolymers were completely soluble in chloroform. The M_n's of the copolymers (5400−12 200) were obviously higher than that of poly(**8**). The specific rotation increased with increasing content of unit **10**.

Table 3. Copolymerization of Monomers 8 and 10[a]

8/**10** in monomer feed (mol/mol)	yield[b] (%)	M_n[c]	M_w/M_n[c]	cis content[d] (%)	$[\alpha]_D$[d,e] (deg)
0/100	95	10500	2.00	100	+1558
10/90	98	10600	2.44	96	+1513
20/80	96	12200	2.02	92	+1461
40/60	98	9200	2.64	n.d.[f]	+1043
50/50	100	8200	2.79	n.d.[f]	+991
60/40	100	7900	2.68	n.d.[f]	+426
70/30	97	6400	3.02	n.d.[f]	+324
80/20	100	5500	3.05	n.d.[f]	+186
90/10	98	5400	2.55	n.d.[f]	+128
100/0	97[g]	3100	1.29	n.d.[f]	0

[a] With (nbd)$Rh^+B^-(C_6H_5)_4$ catalyst in THF at 30 °C for 1 h; $[M]_{total}$ = 0.60 M; $[M]_{total}/[Rh]$ = 100. [b] Precipitated in hexane. [c] Measured by GPC (polystyrenes as the standards; $CHCl_3$ as an eluent). [d] Determined by ^1H NMR in $CDCl_3$ at 50 °C. [e] Measured by polarimetry in $CHCl_3$ at rt (c = 0.080−0.1 g/dL). [f] Could not be determined because of broad singals. [g] Partly soluble in $CHCl_3$.

The UV−vis and CD spectra of poly(**8**-*co*-**10**)s are presented in Figure 3, from where we can see that the copolymer compositions largely affected the UV−vis spectra. More specifically, poly(**8**) and poly(**10**) demonstrated UV−vis absorption peaks around 365 and 400 nm, respectively. If we see Figure 3 starting from poly(**10**), initially a blue shift and then a red shift were observed in the UV−vis absorption peaks of poly(**8**-*co*-**10**)s. Poly(**8**) did not show a CD signal due to the lack of a chiral center. Poly(**10**) showed a CD signal around 400 nm, which implies that it takes a helical structure with predominantly one-handed screw sense.[7g] The CD signals of the copolymers exactly agreed in position with their UV−vis absorption peaks, and both CD signal and UV−vis peak shifted with the change of copolymer compositions. In other words, the composition dependence was observed in both CD and UV−vis spectroscopies. The CD and UV−vis spectra of poly(**8**-*co*-**10**)s in Figure 3 provide enough evidence for us to conclude that the copolymers adopt helices with different pitches. It has been reported that cis−transoidal polyacetylene in a tightly helical form shows the maximum absorption (λ_{max}) at a shorter wavelength than that in a loosely helical one; i.e., the conjugation length of the former is shorter than that of the latter.[11]

The results stated above regarding the shifts of UV−vis absorption and CD signal can be interpreted as follows: As unit **8** increases from 0 to 50% in poly(**8**-*co*-**10**)s, hydrophobic interactions[10] between the pendent groups gradually intensify and in turn lead to tight helical structures. When the content of unit **8** is raised further, steric repulsion between the pendent groups exerts adverse effects and the helices become loose. Consequently, the observed shifts of λ_{max} will appear in the UV−vis absorption and CD signal. However, it still remains unclear about the exact driving force for these copolymers to take helices with different pitches.

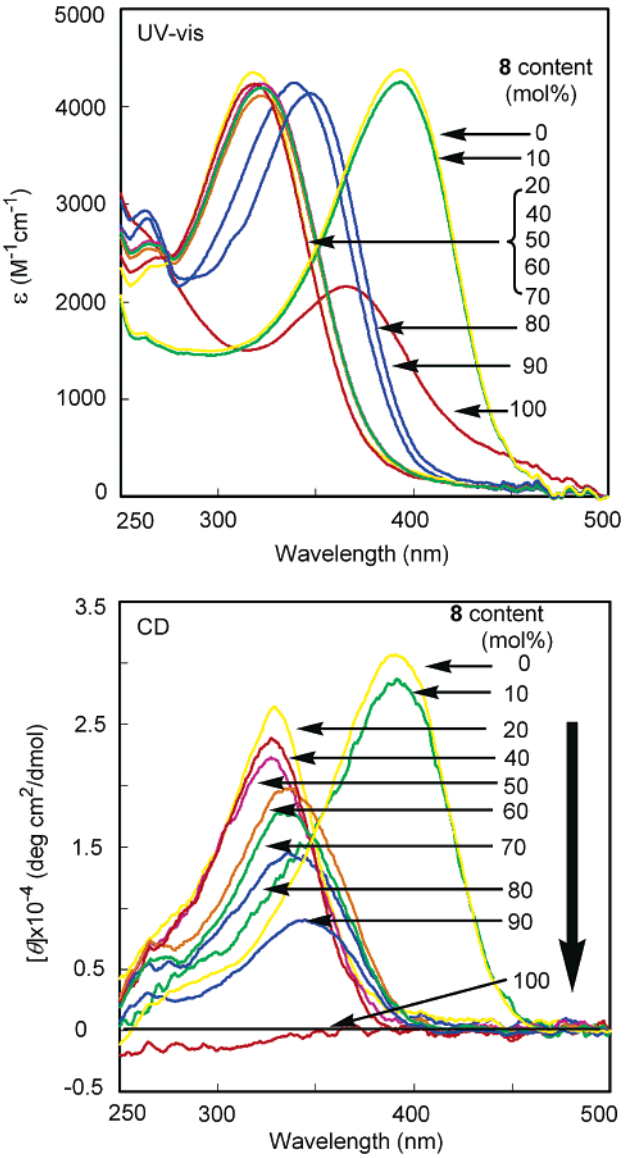

Figure 3. UV−vis and CD spectra of poly(**8**-*co*-**10**)s measured in $CHCl_3$ at 5−55 °C (c = 0.08−0.10 mM; $CHCl_3$-soluble part was used).

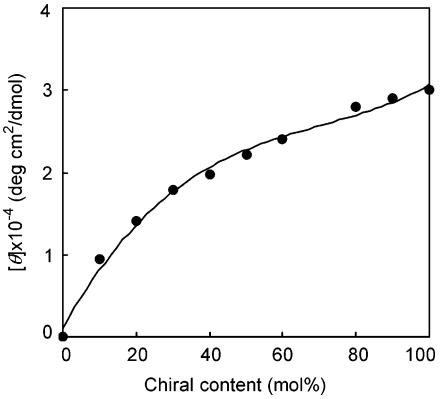

Figure 4. Dependence of the CD intensity on the composition of poly(**8**-*co*-**10**)s. The CD spectra were measured in $CHCl_3$ at 5 °C (c = 0.08−0.10 mM; $CHCl_3$-soluble part was used).

In Figure 4, the CD signal intensities of poly(**8**-*co*-**10**)s are plotted against the content of chiral unit **10**. The intensity increased with the increment of the content of **10** in the copolymers. Special attention should be paid to poly($\mathbf{8}_{0.9}$-*co*-$\mathbf{10}_{0.1}$). Though it contains only 10% of chiral unit **10**, its CD signal intensity reached 10 000 deg cm²/dmol, i.e., one-third that of poly(**10**); thus, the sergeants and soldiers rule[12] was observed in this series of copolymers. It is noteworthy that the chiral unit **10** determines the handedness of the helical sense, while unit **8** largely affects the helical pitches. The synergistic effects between the pendent groups play important roles in the handedness and pitches of the helices.

Table 4. Copolymerization of Monomers 8 and 1[a]

8/**1** in monomer feed (mol/mol)	yield[b] (%)	M_n[c]	M_w/M_n[c]
0/100	85	6300	2.85
10/90	100	8200	2.51
20/80	98	9100	2.19
30/70	99	7000	2.45
40/60	97	6800	2.25
50/50	100	6000	2.31
60/40	99	5300	2.61
80/20	100	4800	2.78
100/0	97[d]	3100	1.29

[a] With (nbd)$Rh^+B^-(C_6H_5)_4$ catalyst in THF at 30 °C for 1 h; $[M]_{total}$ = 0.60 M; $[M]_{total}/[Rh]$ = 100. [b] Precipitated in hexane. [c] Measured by GPC (polystyrenes as the standards; $CHCl_3$ as an eluent). [d] Partly soluble in chloroform.

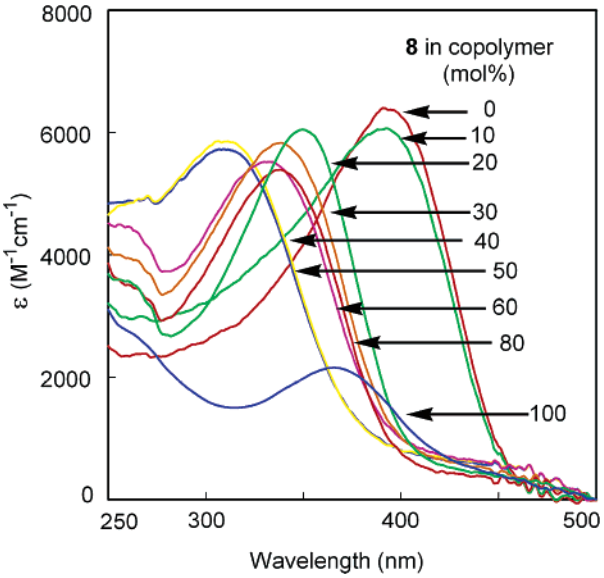

Figure 5. Composition dependence of the UV−vis spectra of poly(**8**-*co*-**1**)s measured in $CHCl_3$ at 5 °C (c = 0.08−0.10 mM; $CHCl_3$-soluble part was used).

Achiral/Achiral Copolymers, Poly(8-*co*-1)s and Poly(8-*co*-9)s. Copolymerizations of monomer **8** with either monomer **1** or **9**, whose structures are presented in Scheme 1, were carried out in order to improve the polymer solubility, increase the M_n of poly(**8**), and further elucidate the secondary structures of the synthesized achiral/achiral copolymers. Table 4 shows the copolymerization results of monomers **8** and **1**. We can see that the copolymerizations proceeded smoothly, and all the copolymers totally dissolved in chloroform and had increased M_n's in comparison with poly(**8**).

The UV−vis spectra of poly(**8**-*co*-**1**)s are illustrated in Figure 5. The UV−vis absorption peaks appeared at different wavelengths for the poly(**8**-*co*-**1**)s, just like poly(**8**-*co*-**10**)s in Figure 3. To make it clearer, we plotted the relationship between the wavelengths (λ_{max}) of the maximum UV−vis absorption and the compositions of the (co)polymers in Figure 6. The λ_{max}'s of poly(**1**) and poly(**8**) were observed at 396 and 365 nm, respectively.

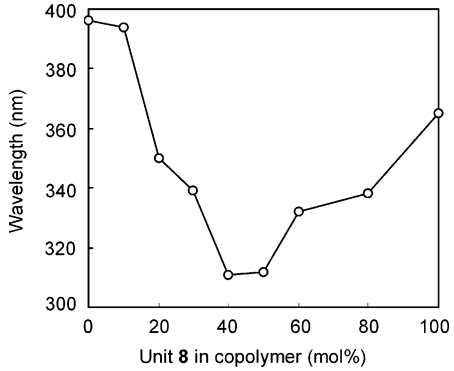

Figure 6. Plot of the wavelengths (λ_{max}) of the maximum UV−vis absorption against the contents of unit **8** in poly(**8**-*co*-**1**)s. The UV−vis spectra were measured in $CHCl_3$ (c = 0.08−0.10 mM; $CHCl_3$-soluble part was used).

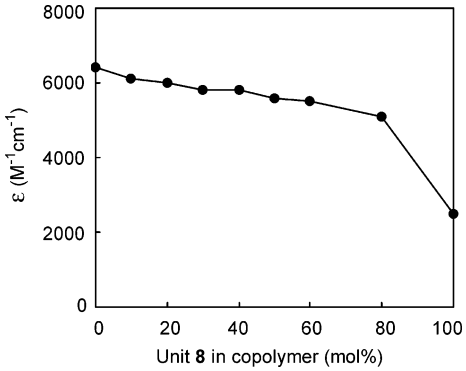

Figure 7. Dependence of molar absorption (ϵ) in the UV−vis spectrum on the content of unit **8** in poly(**8**-*co*-**1**)s. The UV−vis spectra were measured in $CHCl_3$ (c = 0.08−0.10 mM; $CHCl_3$-soluble part was used).

A blue shift of λ_{max} occurred with increasing content of unit **8** in the copolymers up to 40%. In contrast, a red shift was observed with further increasing content of unit **8**. Considering the continuous blue and red shifts of the UV−vis absorption in these (co)polymers, a similar behavior to the case of poly(**8**-*co*-**10**)s, we think that all the absorption peaks appearing in Figure 5 are based on helices, and the shift of the λ_{max} is caused by varying pitches of the helices, which depends on the compositions of the (co)polymers.

Figure 7 presents the dependence of UV−vis absorption intensities (ϵ) on the compositions of the (co)polymers. The ϵ became smaller as the content of unit **8** increased. For instance, the values of ϵ were 6400, 5600, and 2500 M^{-1} cm^{-1} for poly(**1**), poly($\mathbf{8}_{0.5}$-*co*-$\mathbf{1}_{0.5}$), and poly(**8**), respectively. This implies that too large steric repulsion between the pendent groups is unfavorable for the polymers to take stable helical structure. Namely, with the increment of unit **8**, the steric repulsion between the pendent groups becomes larger, and the helix content of the (co)polymer decreases gradually, which results in the decrease of ϵ. Another possible reason for the reduction of ϵ is the M_n's of the (co)polymers. However, this should not be the case since poly(*N*-propargylamides) with even lower M_n's (<2500) can show quite high helix contents.[7c]

The helices formed in the (co)polymers were quite stable to heating. Take poly($\mathbf{8}_{0.5}$-*co*-$\mathbf{1}_{0.5}$) as an example, whose UV−vis spectra are shown in Figure 8. Even when the temperature was raised from 5 to 55 °C, the intensity of the absorption peak decreased only slightly.

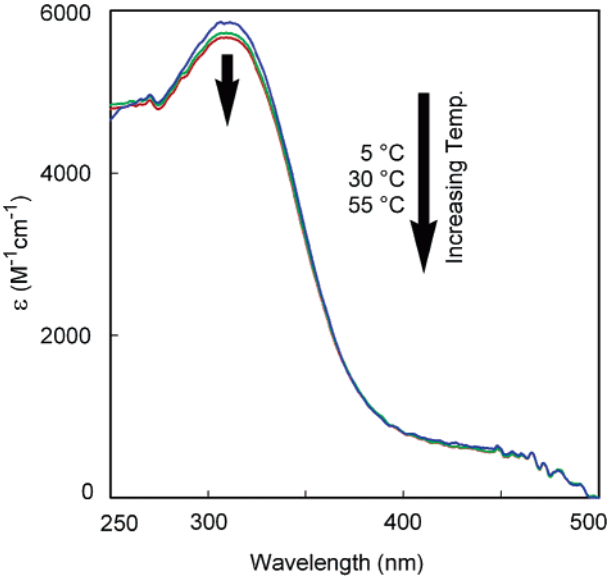

Figure 8. Effect of temperature on the UV−vis spectra of poly($\mathbf{8}_{0.5}$-*co*-$\mathbf{1}_{0.5}$) measured in $CHCl_3$ (c = 0.1 mM).

Table 5. Copolymerization of Monomers 8 and 9[a]

8/9 in monomer feed (mol/mol)	yield[b] (%)	M_n[c]	M_w/M_n[c]	cis content[d] (%)
0/100	85	18 300	2.12	92
20/80	98	23 000	2.09	98
40/60	97	22 600	2.06	n.d.[f]
60/40	99	15 000	2.47	n.d.[f]
80/20	100	12 000	2.76	n.d.[f]
100/0	97[e]	3 100	1.29	n.d.[f]

[a] With (nbd)$Rh^+B^-(C_6H_5)_4$ catalyst in THF at 30 °C for 1 h; $[M]_{total}$ = 0.60 M (except monomer **9**, whose concentrated is 1.0 M); $[M]_{total}/[Rh]$ = 100. [b] Precipitated in hexane. [c] Measured by GPC (polystyrenes as the standards; $CHCl_3$ as an eluent; in the case of poly(**9**), THF as an eluent). [d] Determined by ^1H NMR in $CDCl_3$ at 50 °C. [e] Partly soluble in chloroform. [f] Could not be determined because of broad signals.

Similar results were also obtained in the other poly(**8**-*co*-**1**)s.

Copolymerizations of monomer **8** with **9** were also performed, and Table 5 gives the copolymerization results. All the copolymers had moderate M_n's (12 000−23 000) and were soluble in chloroform. Thus, the solubility of the copolymers was effectively improved, and the M_n's were remarkably increased. The UV−vis spectra of poly(**8**-*co*-**9**)s are presented in Figure 9. Poly(**8**) and poly(**9**) showed absorption peaks around 365 and 400 nm, respectively, while the copolymers did at different wavelengths. The copolymers with 20%, 40%, and 60% of unit **8** showed absorption peaks around 320 nm, while poly($\mathbf{8}_{0.8}$-*co*-$\mathbf{9}_{0.2}$) showed a peak around 345 nm. Thus, Figure 9 demonstrates composition dependence of the UV−vis absorption.

Considering the CD data (Figure 3) along with the UV−vis spectra, it is very reasonable to think that all the UV−vis absorption peaks in Figures 3, 5, and 9 are based on helical structures and not on random coil ones because they showed the common feature of composition dependence. Consequently, we can conclude from UV−vis and CD spectroscopies that all of poly(**8**-*co*-**10**)s, poly(**8**-*co*-**1**)s, and poly(**8**-*co*-**9**)s form helices with different pitches depending on the copolymer compositions. Comparing the UV−vis spectra of poly(**8**-*co*-**10**)s, poly(**8**-*co*-**1**)s, and poly(**8**-*co*-**9**)s, large differences are observed in the variations of helical pitches, even though the

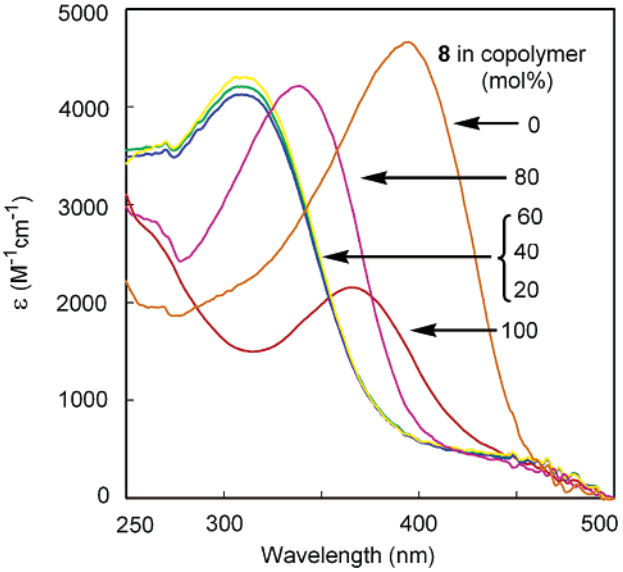

Figure 9. UV−vis spectra of poly(**8**-*co*-**9**)s measured in $CHCl_3$ at 5 °C (c = 0.08−0.10 mM; $CHCl_3$-soluble part was used).

composition dependence is a common phenomenon among these copolymers. It is assumed that the repulsion between the pendent groups in the copolymers is different in magnitude, which results in the different pitches of the helices, and in turn, the UV−vis absorption peaks are observed at different wavelengths.

Conclusion

Five *N*-propargylacetamide and -propaneamide monomers with different numbers of phenyl groups (**4**−**8**) were newly synthesized. Monomers **6** and **7** smoothly underwent polymerization with an Rh catalyst to provide polymers with moderate molecular weights and good solubility in chloroform. On the other hand, monomers **4**, **5**, and **8** gave polymers partly soluble in solvents. Poly(**4**) formed a helical structure, while poly(**5**) hardly did, presumably because of its too crowded pendent groups. Poly(**8**) formed helices with pitches different from other poly(*N*-propargylamides), which probably depends on intramolecular hydrogen bonds, steric repulsion between the pendent groups, and hydrophobic interactions between the crowded phenyl groups. Copolymers of monomer **8** with chiral and achiral monomers exhibited UV−vis absorption peaks and CD signals [poly(**8**-*co*-**10**)s] at various wavelengths, showing that the resulting helices possess different pitches that depend on the combination of the comonomer and copolymer composition.

References and Notes

(1) For conjugated polymers, see: (a) Masuda, T.; Sanda, F. In *Handbook of Metathesis*; Grubbs, R. H., Ed.; Wiley-VCH: Weinheim, 2003; Vol. 3; Chapter 3.11. (b) Capitani, D.; Laurienzo, P.; Malinconico, M.; Proietti, N.; Roviello, A. *J. Polym. Sci., Part A: Polym. Chem.* **2003**, *41*, 3916. (c) Tabata, M.; Sone, T.; Mawatari, Y.; Yonemoto, D.; Miyasaka, A.; Fukushima, T.; Sadahiro, Y. *Macromol. Symp.* **2003**, *192*, 75. (d) Yashima, E.; Maeda, K. *ACS Symp. Ser.* **2002**, *812*, 41. (e) Heeger, A. J. *Rev. Mod. Phys.* **2001**, *73*, 681. (f) Nagai, K.; Masuda, T.; Nakagawa, T.; Freeman, B. D.; Pinnau, I. *Prog. Polym. Sci.* **2001**, *26*, 721. (g) McQuade, D. T.; Pullen, A. E.; Swager, T. M. *Chem. Rev.* **2000**, *100*, 2537. (h) Kraft, A.; Grimsdale, A. C.; Holmes, A. B. *Angew. Chem., Int. Ed.* **1998**, *37*, 402. (i) Masuda, T. Acetylenic Polymer. In *Polymeric Material Encyclopedia*; Salamone, J. C., Ed.; CRC Press: New York, 1996; Vol. 1, p 32.

(2) (a) Tang, H. Z.; Fujiki, M.; Sato, T. *Macromolecules* **2002**, *35*, 6439. (b) Tang, H. Z.; Fujiki, M.; Motonaga, M. *Polymer* **2002**, *43*, 6213. (c) Oda, M.; Nothofer, H. G.; Lieser, G.; Scherf, U.; Meskers, S. C. J.; Neher, D. *Adv. Mater.* **2000**, *12*, 362. (d) Oda, M.; Meskers, S. C. J.; Nothofer, H. G.; Scherf, U.; Neher, D. *Synth. Met.* **2000**, *111*−*112*, 575.

(3) (a) Maeda, K.; Morino, K.; Yashima, E. *Macromol. Symp.* **2003**, *201*, 135. (b) Goto, H.; Zhang, H. Q.; Yashima, E. *J. Am. Chem. Soc.* **2003**, *125*, 2516. (c) Yashima, E.; Maeda, K.; Okamoto, Y. *Nature (London)* **1999**, *399*, 449.

(4) (a) Sato, I.; Kadowaki, K.; Urabe, H.; Jung, J. H.; Ono, Y.; Shinkai, S.; Soai, K. *Tetrahedron Lett.* **2003**, *44*, 721. (b) Reetz, M. T.; Beuttenmuller, E. W.; Goddard, R. *Tetrahedron Lett.* **1997**, *38*, 3211. (c) Guo, C.; Qiu, J.; Zhang, X.; Verdugo, D.; Larter, M. L.; Christie, R.; Kenney, P.; Walsh, P. J. *Tetrahedron* **1997**, *53*, 4145. (d) Ebrahim, S.; Wills, M. *Tetrahedron: Asymmetry* **1997**, *8*, 3163.

(5) (a) Baldwin, R. L.; Rose, G. D. *Trends Biochem. Sci.* **1999**, *24*, 26. (b) Dobson, C. M.; Sali, A.; Karplus, M. *Angew. Chem., Int Ed.* **1998**, *37*, 868.

(6) For synthetic helical polymers, see: (a) Yashima, E.; Maeda, K.; Nishimura, T. *Chem.*−*Eur. J.* **2004**, *10*, 42. (b) Nakano, T.; Okamoto, Y. *Chem. Rev.* **2001**, *101*, 4013. (c) Green, M. M.; Park, J. W.; Sato, T.; Teramoto, A.; Lifson, S.; Selinger, R. L. B.; Selinger, J. V. *Angew. Chem., Int. Ed.* **1999**, *38*, 3138. (d) Rowan, A. E.; Nolte, R. J. M. *Angew. Chem., Int. Ed.* **1998**, *37*, 63. (e) Pu, L. *Acta Polym.* **1997**, *48*, 116.

(7) (a) Deng, J.; Tabei, J.; Shiotsuki, M.; Sanda, F.; Masuda, T. *Macromolecules* **2004**, *37*, 1891. (b) Deng, J.; Tabei, J.; Shiotsuki, M.; Sanda, F.; Masuda, T. *Macromol. Chem. Phys.* **2004**, *205*, 1103. (c) Deng, J.; Tabei, J.; Shiotsuki, M.; Sanda, F.; Masuda, T. *Macromolecules* **2004**, *37*, 5149. (d) Tabei, J.; Nomura, R.; Sanda, F.; Masuda, T. *Macromolecules* **2003**, *36*, 8603. (e) Nomura, R.; Nishiura, S.; Tabei, J.; Sanda, F.; Masuda, T. *Macromolecules* **2003**, *36*, 5076. (f) Nomura, R.; Tabei, J.; Nishiura, S.; Masuda, T. *Macromolecules* **2003**, *36*, 561. (g) Tabei, J.; Nomura, R.; Masuda, T. *Macromolecules* **2002**, *35*, 5405. (h) Nomura, R.; Tabei, J.; Masuda, T. *Macromolecules* **2002**, *35*, 2955. (i) Nomura, R.; Tabei, J.; Masuda, T. *J. Am. Chem. Soc.* **2001**, *123*, 8430. (j) Deng, J.; Tabei, J.; Shiotsuki, M.; Sanda, F.; Masuda, T. *Macromolecules* **2004**, *37*, 7156.

(8) Schrock, R. R.; Osborn, J. A. *Inorg. Chem.* **1970**, *10*, 2339.

(9) (a) Tabata, M.; Sone, T.; Sadahiro, Y. *Macromol. Chem. Phys.* **1999**, *200*, 265. (b) Masuda, T. In *Catalysis in Precision Polymerization*; Kobayashi, S., Ed.; Wiley: Chichester, 1997; Chapter 2.4.

(10) (a) Blokzijl, W.; Engberts, J. B. F. N. *Angew. Chem., Int. Ed. Engl.* **1993**, *32*, 1545. (b) O'Neill, J. C., Jr.; Matthews, C. R. *J. Mol. Biol.* **2000**, *295*, 737. (c) Methenitis, C.; Morcellet, J.; Pneumatikakis, G.; Morcellet, M. *Macromolecules* **1994**, *27*, 1455. (d) Sneddon, S. F.; Tobias, D. J. *Biochemistry* **1992**, *31*, 2842.

(11) Percec, V.; Obata, M.; Rudick, J.; De Binod, B.; Glodde, M.; Bear, T. K.; Magonov, S. N.; Balagurusamy, V. S. K.; Heiney, P. A. *J. Polym. Sci., Part A: Polym. Chem.* **2002**, *40*, 3509.

(12) (a) Prince, R. B.; Moore, J. S.; Brunsveld, L.; Meijer, E. W. *Chem.*−*Eur. J.* **2004**, *7*, 4150. (b) Prins, L. J.; Timmerman, P.; Reinhoudt, D. N. *J. Am. Chem. Soc.* **2001**, *123*, 10153. (c) Palmans, A. R. A.; Vekemans, J. A. J. M.; Havinga, E. E.; Meijer, E. W. *Angew. Chem., Int. Ed. Engl.* **1997**, *36*, 2648. (d) Green, M. M.; Reidy, M. P.; Johnson, R. D.; Darling, G.; O'Leary, D. J.; Willson, G. *J. Am. Chem. Soc.* **1989**, *111*, 6452.

MA048177R